KSÜ Mühendislik Bilimleri Dergisi, 27(2), 2024
Araştırma Makalesi

KSU J Eng Sci, 27(2), 2024
Research Article

Kahramanmaras Sutcu Imam University
Journal of Engineering Sciences

Geliş Tarihi : 10.09.2023
Kabul Tarihi :12.01.2024

Received Date : 10.09.2023
Accepted Date : 12.01.2024

EVALUATION OF BEARING CAPACITY INCREASE FOR WOVEN GEOTEXTILE REINFORCED SOILS IN TERMS OF WIDTH OF FOOTING

ÖRGÜLÜ GEOTEKSTİL İLE GÜÇLENDİRİLMİŞ ZEMİNLER İÇİN TAŞIMA KAPASİTESİ ARTIŞININ TEMEL GENİŞLİĞİ AÇISINDAN DEĞERLENDİRİLMESİ

Bayram ATEŞ[1*] (ORCID: 0000-0002-1251-7053)
Erol ŞADOĞLU[1] (ORCID: 0000-0003-3757-5126)

[1] Karadeniz Technical University, Department of Civil Engineering, Trabzon, Türkiye

*Sorumlu Yazar / Corresponding Author: Bayram ATEŞ, bayramates61@hotmail.com

ABSTRACT

If it is understood that a soil medium cannot safely support the planned structure from the point of bearing capacity and settlement, various options can be applied in geotechnical engineering. These are relocation of the structure, usage of deep foundation, stabilisation of the soil, substitution of weak soil with well-graded coarse-grained soil by compaction, usage of geosynthetics, etc. These alternatives are evaluated according to the cost and availability of necessary materials and equipment. Geotextiles, one of the geosynthetic products, have been widely used for soil reinforcement recently. Therefore, the study intends to specify the soil's bearing capacity increase with geotextile and its dependence on footing width. For this aim, a testing apparatus has been produced, and the experiments have been conducted with a strip footing model on soil with various relative densities. Besides, this test setup was simulated with PLAXIS 2D software depending on the finite element method (FEM), and numerical analyses were performed. The numerical results were compared with the laboratory tests to verify parameters of M-C material model. Consequently, the study stated that the relative density of the sand, footing width, and reinforcement layer are significant factors for the bearing capacity increase of granular soils.

Keywords: Geotextile, reinforced soil, model test, numerical analysis, width of footing

ÖZET

Bir zemin ortamının, düşünülen yapıyı taşıma gücü ve oturma açılarından güvenli olarak taşıyamayacağı tespit edilirse, geoteknik mühendisliği açısından alternatif yollara başvurulabilir. Bunlar; yapının yerinin değiştirilmesi, derin temel kullanılması, zeminin stabilizasyonu, kötü zeminin kaldırılarak, yerine iyi derecelenmiş iri taneli zeminin kompaksiyonla yerleştirilmesi, geosentetik kullanılması vb. dir. Bu seçenekler; maliyet, eldeki araç-gereç durumuna göre değerlendirilir. Geosentetik ürünlerden biri olan geotekstiller son yıllarda zemin güçlendirilmesinde yaygın olarak kullanılmaktadır. Bu çalışmada geotekstille güçlendirilmiş zeminlerin taşıma kapasitesi artışının ve bunun temel genişliği ile ilişkisinin tespit edilmesi hedeflenmiştir. Bu bağlamda, bir deney mekanizması kurulmuş ve çeşitli sıkılıklarda yerleştirilmiş kum zemine oturan temeller yardımı ile deneyler yürütülmüştür. İlave olarak; mevcut deney düzeneği sonlu elemanlar tabanında çözümleme yapan PLAXIS 2D programı ile modellendi ve sayısal analizler yapıldı. Böylece bu numerik sonuçlar model deneylerden elde edilen sonuçlar ile M-C malzeme modeli parametrelerini doğrulamak için karşılaştırıldı. Sonuç olarak, zeminin sıkılığı, donatı tabakası ve temel genişliği, granüler zeminlerin taşıma gücü artışı üzerinde etkili parametreler olduğu belirlenmiştir.

Anahtar Kelimeler: Geotekstil, güçlendirilmiş zemin, model deney, nümerik analiz, temel genişliği

ToCite: ATEŞ, B., & ŞADOĞLU, E., (2024). EVALUATION OF BEARING CAPACITY INCREASE FOR WOVEN GEOTEXTILE REINFORCED SOILS IN TERMS OF WIDTH OF FOOTING. *Kahramanmaraş Sütçü İmam Üniversitesi Mühendislik Bilimleri Dergisi*, 27(2), 325-339.

INTRODUCTION

Geosynthetics have significantly been preferred in geotechnical applications to advance the bearing capacity (BC) of soils and to decrease shallow footings' settlement (s) for fifty years. Geotextiles are one of the most preferred geosynthetic materials used in these applications. There are differences in the BC and failure behaviour of the sand with reinforcement and sand without reinforcement. Failure surfaces, and sand movements of the footing on the soil without reinforcement are illustrated in Fig. 1 (a). A wedge under the footing occurs with the loading of the footing, and then the wedge moves downward with the footing. Shear surfaces that can be accepted as approximately symmetric formed on both sides of the symmetry axis. The failure of the reinforced soil is similar to the soil without reinforcement case (see Fig 1 (b)). In the failure mechanism of the reinforced soil, a soil wedge (trapezoidal+triangular) occurs under the footing, moves downwards with the footing, and pushes adjacent soil towards the sides (Takemura et al., 1992; Michalowski and Shi, 2003; Şadoğlu and Uzuner, 2010; Xu et al., 2019; Venkateswarlu et al., 2020; Gao et al., 2022). Heaves occur at the sides of the footing in dense soil.

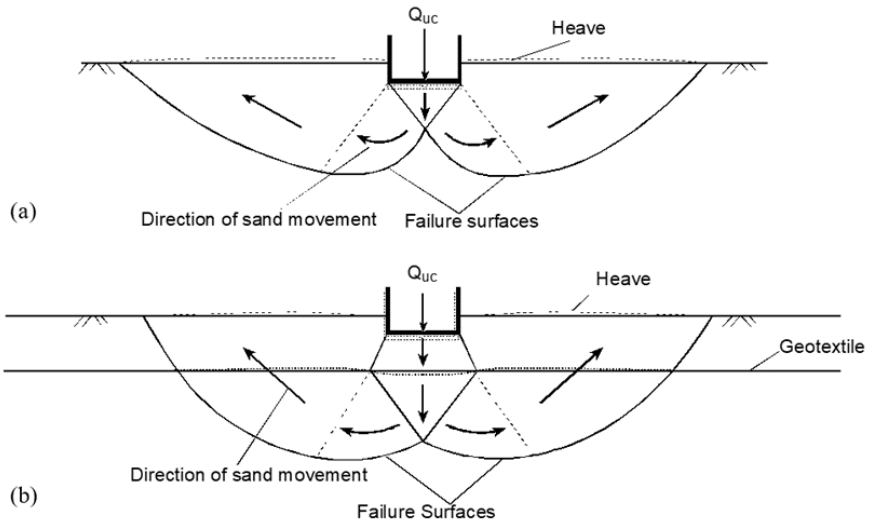

Figure 1. Failure Mechanism in Granular Soil **a.** Soil Without Reinforcement **b.** Soil with Reinforcement (Takemura et al., 1992)

Many researchers have performed theoretical, numerical, and laboratory tests to determine the importance of reinforcement materials in terms of enhancing BC. The load-settlement responses of the foundations on reinforced soil have been engaged attention for a long time by many researchers (Adams and Collin, 1997; Wayne et al., 1998; Michalowski, 2004; Patra et al., 2006; Ghazavi and Lavasan, 2008; Lavasan and Ghazavi, 2012; Ateş and Şadoğlu, 2014; Ateş and Şadoğlu, 2020; Kahraman et al., 2022). The improvement of the ultimate bearing capacity (Q_u) of the footing on the reinforced soil is, as a rule, presented by using a non-dimensional parameter that is called as bearing capacity ratio (BCR) (Binquet and Lee, 1975; Guido et al., 1986; Omar et al., 1993; Patra et al., 2005; Lai and Yang, 2017; Saha Roy and Deb, 2017; Wang et al., 2018; Xu et al., 2018; Useche-Infante et al., 2019; Hussein et al., 2019). The ratio of ultimate bearing capacity is determined by the following equation:

$$BCR_u = Q_{u,\,reinf}/Q_{u,\,unreinf} \quad (1)$$

The following equation specifies the bearing capacity rate (BCR_s) for a given settlement:

$$BCR_s = Q_{reinf}/Q_{unreinf} \quad (2)$$

Asakereh et al. (2013) performed experiments on a small-scale foundation on unreinforced and reinforced sand. The reinforcement layer numbers were examined in terms of cyclic load and cycle number. This study demonstrates that the settlement values of the foundation enhance quickly during the initial loading. Abu-Farsakh et al. (2013) carried out small-scale experiments to study the effect of reinforcement on the advancement in the BC of the foundation soil bed. As a result of these tests, it has been reported that design parameters such as depth and length of first reinforcement and soil type are effective parameters in improving the BC of the reinforced soil. Chakraborty and Kumar (2014) studied the Q_u of a circular foundation resting on the reinforced soil. In these studies, as a method,

finite elements were specified and investigated the limit analysis for a foundation resting on soil with reinforcement. Eventually, the optimal depth and the diameters of the reinforcements have been determined to ensure maximum BC of the foundation soil bed. It has also been seen that two reinforcement layers instead of a single reinforcement layer provide a significant enhancement in the BC of this circular foundation. These studies demonstrate the significance of the reinforcement for the BC of the foundation soil bed. Even though many researches were performed to examine the effects of various design variables on the performance of reinforced soil, very few studies were carried out to determine the effects of footing width and relative density on the bearing capacity of reinforced soils with geotextile. The main purpose of this study is to reveal the bearing capacity increase of the soil reinforced with polypropylene fiber-originated woven geotextile and its dependence on the footing width and the relative density with 1-g physical model tests and numerical analysis. In this context, a testing apparatus was first connected in conformity with plane strain condition, and the tests on strip footing resting on granular soils reinforced with geotextile were conducted. Then, the test setup was simulated with PLAXIS 2D software based on the FEM, and numerical analyses were performed.

MATERIAL AND METHODS

Experimental Study

Scaled tests are made a choice in many geotechnical investigations because of their cost-efficiency, time-saving, and applicability. Moreover, failure surface geometry in most reinforced soil studies was investigated with these tests. Within this scope, a testing apparatus has been carried out, and loading tests have been performed with the help of the strip footing on the sand. The test setup includes a testing tank, strip footing, linear variable displacement transducers (LVDT), a hydraulic jack as the loading apparatus, a load cell, a computer, a data logger and sand.

Testing Tank

The testing tank is a rectangular hollow prism, and the internal sizes of the test tank are 960 x 200 x 650 mm^3 (Moroglu et al., 2005; Ateş and Şadoğlu, 2014; Ateş and Şadoğlu, 2020; Chen et al., 2021). The tank's frame used in laboratory tests was made of steel profiles. The rigidity of the tank is ensured by welding steel supports to certain points of the test tank (see Figure 2). Ideally, thin latex sheets should be placed on the internal faces of the lightly lubricated glass plates to achieve almost frictionless side faces. This application has difficulties due to the movements of the sand mass in different directions. The sand is in contact with glass faces directly in this experimental work. Kirkpatrick and Uzuner (1975) showed that the effect of side friction between glass sides and sand on bearing capacity is less than 10% for a surface footing sitting on medium-dense sand. The conditions of this experimental work are close to the conditions of the work done by Kirkpatrick and Uzuner (1975). Moreover, the effect of side friction is approximately eliminated in this experimental work due to the usage of the bearing capacity ratio (BRC), bearing capacity increase (%) and settlement ratio instead of the ultimate loads.

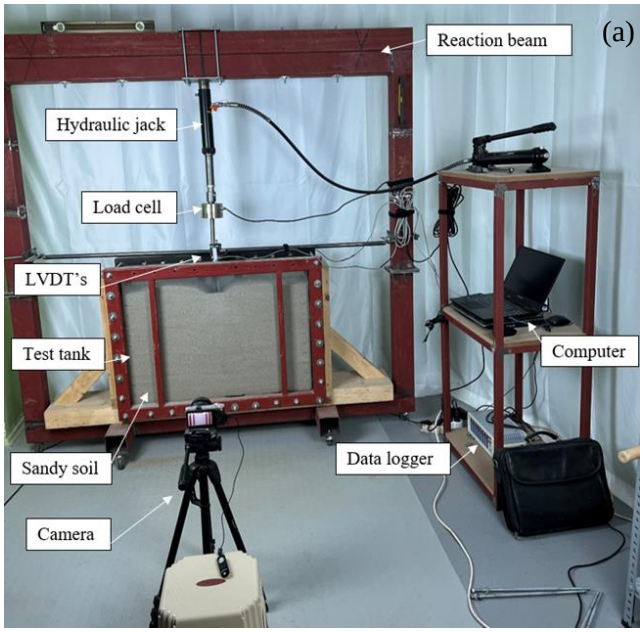

Figure 2. Test Setup **a.** A General View **b.** Schematic Diagram

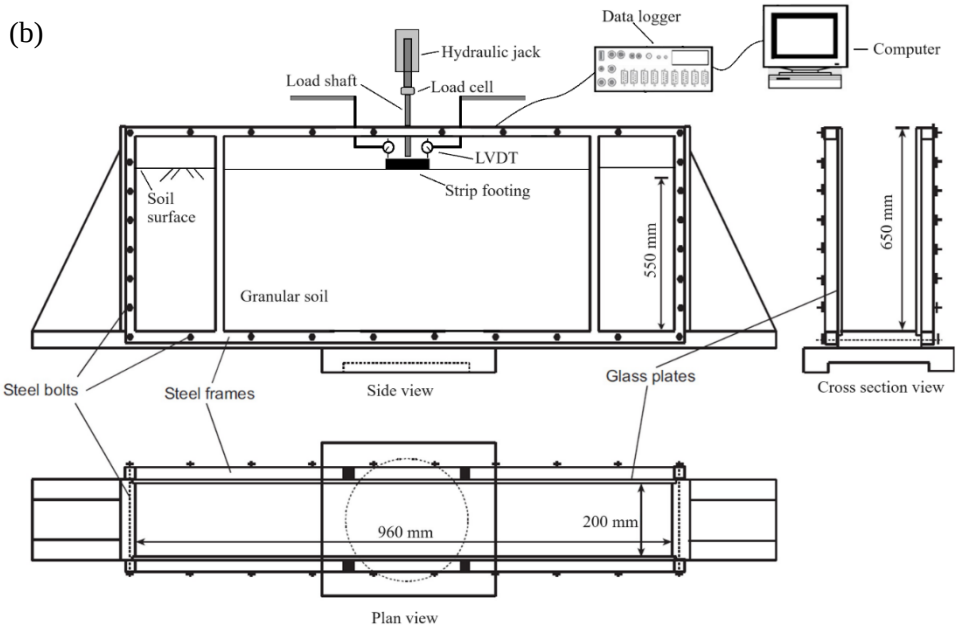

Figure 2. Test Setup **a.** A General View **b.** Schematic Diagram

Kirkpatrick and Yanikian (1975) proposed that ε_y=0 should be less than 0.1% for plane strain models. Two steel frames made of hollow sections were produced and connected with steel bolts along the sides of the frames. Steel elements made of solid profiles were welded in the middle part of the frames to prevent the deformation of the glass plates. The surface of the steel frame that the glass plates touched was produced to be almost perfectly plane so that no glass was broken during the tests. Two dial gauges were placed on the external faces of the glass plates to measure lateral deformations. Measured horizontal displacements revealed that the horizontal strains of the sides were found to be considerably less than 0.1% in the tests.

Small-Scale Foundation

A literature survey was researched, and trial tests were performed to specify the sizes of the footing used in the experimental study. The strip foundation model's width (B) was chosen as 100 mm (Kargar et al., 2016; Chen et al., 2019). A coarse sandpaper was mounted on the base of the strip footing to ensure full friction conditions (see Figure 3).

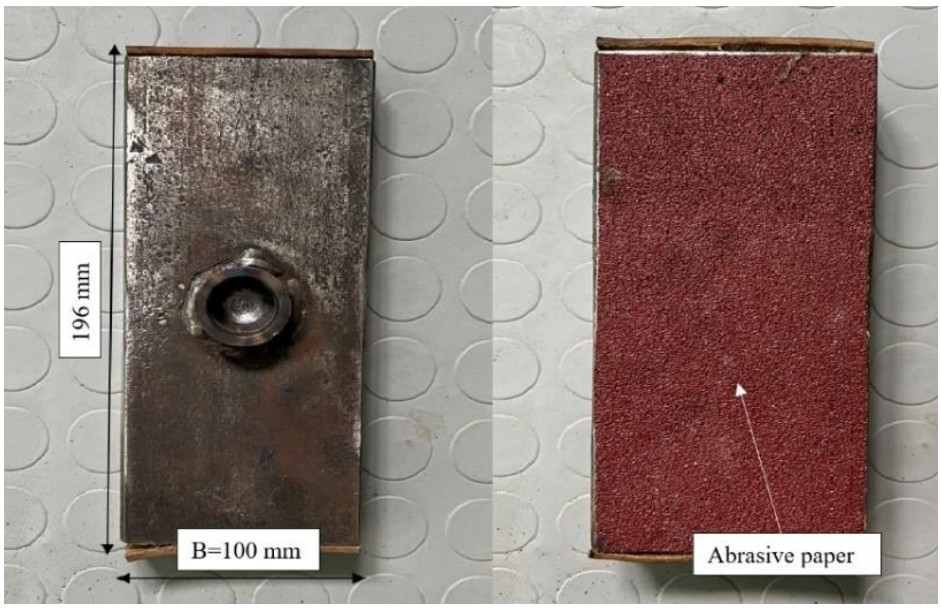

Figure 3. Model Strip Footing

Reinforcement Layer

The widths of geotextile sheets used as reinforcements were equal to the internal width of the test tank (200 mm) prepared for the experiments (see Figure 4). The tensile strength of the geotextile was determined according to ASTM 4595-17 (2017) (see Table 1).

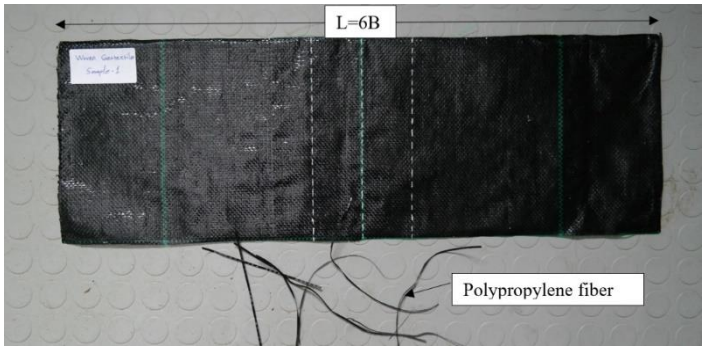

Figure 4. A General View of Woven Geotextile

Table 1. Specification of Geosynthetic Reinforcement

Property	Unit	Value
Material Property	-	Polypropylene
Type	-	Woven
Ultimate Tensile Strength	kN/m	20
Tensile Strength at %2 strain	kN/m	4.14
Tensile Strength at %5 strain	kN/m	7.83
Mass per Unit Area	g/m^2	100

Sand

The soil was sand obtained from the southern coast of the Black Sea. The particle size distribution of the sand was detected regarding ASTM D-6913 (2017) (see Figure 5). The particle size range of the sand was selected too small compared to the dimensions of the footing so as to avoid scale effect. Toyosawa et al. (2013) investigated the particle size effect on the bearing capacity of circular model footing with centrifugal tests. It was found if the ratio of footing diameter to mean particle size (D_{50}) is more than 50 for a circular surface footing, the effect of particle size on bearing capacity is neglectable. Therefore, the ratio of the width of the footing model to the mean particle size of the sand was selected as 125 (B/D_{50}=100) in this study.

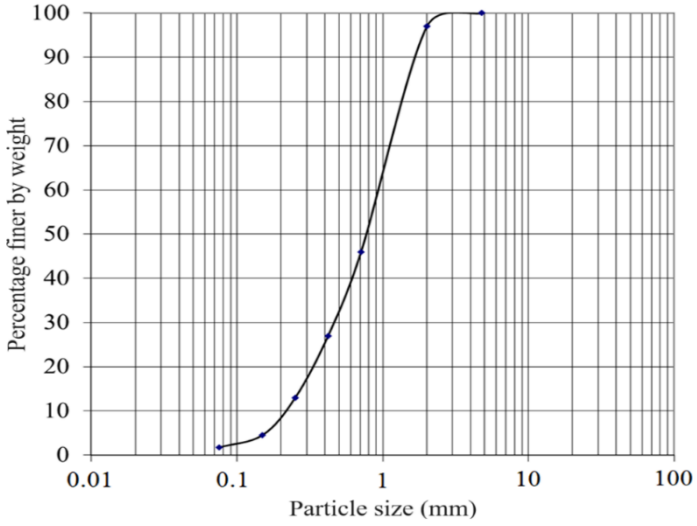

Figure 5. Particle Size Distribution Curve

The sand specification is illustrated in Table 2. The dry unit weights were detected for loose and dense cases separately. Similarly, the internal friction angles for D_r=0.30 and 0.70 were obtained by the shear box test.

Table 2. The Sand Specification

Property	Unit	Value
Grain Specific Gravity, *Gs* (ASTM D-854, 2006)	-	2.74
Maximum Dry Density, ρ_{dmax} (ASTM D4254-16, 2016)	Mg/m^3	1.82
Minimum Dry Density, ρ_{dmin} (ASTM D4253-16, 2016)	Mg/m^3	1.39
Effective Diameter, D_{10}	mm	0.21
D_{30}	mm	0.56
D_{60}	mm	0.90
Coefficient of Uniformity, C_u	-	2.14
Coefficient of Curvature, C_c	-	0.83
Internal Friction Angle, ϕ (D_r=0.70) (ASTM D3080M-11, 2011)	Degrees	45.00
Internal Friction Angle, ϕ (D_r=0.30) (ASTM D3080M-11, 2011)	Degrees	38.00

Loading and Data Equipments

A hydraulic jack (100 kN) was integrated into the reaction beam of the testing tank and was used to apply vertical loading. A load cell was incorporated at the end of the hydraulic jack. The magnitude of the loading was measured precisely with the load cell with a capacity of 20 kN. LVDT, which can measure displacements up to 50 mm, was used to determine the displacement of the strip footing. The data measured by the load cell and the LVDTs were transferred to the computer using the data logger.

Test Procedure

The soil required for a 50 mm layer was poured into the test tank at a close distance (30-40 mm) to avoid compaction in the case of the loose sand (D_r = 0.3, ρ_d = 1.49 Mg/m^3). However, the sand for a layer was compacted with a small compaction device for dense sand (D_r = 0.7, ρ_d = 1.66 Mg/m^3). The compaction device is specially designed for the study and produced by using a hammer drill. The surface of the sand was made horizontal with a water balance, and thus the sand was homogeneously placed. The height of the sand layer was controlled by the horizontal lines indicating the layer thickness on the internal surfaces of the tank. In addition, the geotextile reinforcement was placed in the desired location in this process (see Figure 6). The dry density of the deposited sand (or its relative density) in the tank was calculated by weighing the sand mass removed from the tank. Before the actual tests were performed, several sand depositions in the tank were made. Good agreement was found in these trials. The error in relative density was calculated to be less than 1% in these trials. The density of the sand was checked by locating six containers at three different depths on both the left and right sides of the centerline of the tank in order to ensure the uniformity of the layers. It was seen that the variation in density was almost negligible.

Figure 6. Placement of Sand and Geotextile

The LVDTs were mounted on both sides of the strip footing, and the load cell was integrated into the hydraulic jack (see Figure 7). The initial values of the LVDTs and load cell were reset to zero. The strip foundation model was loaded into the sand at a constant velocity. Variation of bearing capacity with load velocity was investigated by Vesic et al. (1965) for 101.6 mm diameter rigid rough model footing placed on the surface of a dense sand. The minimum bearing capacity was measured with the loading velocity of 0.1 mm/s. Therefore, this loading velocity was applied during the experiments. While the foundation was loaded into the soil, the perpendicularity of the foundation was tracked using water balance. A constant loading rate was carried out until the specific settlement (s = B/4) was achieved.

Figure 7. The Starting of Vertical Loading

Test Program

Design variables of horizontal soil with reinforcement and soil without reinforcement are shown in Figure 8. Some parameters were investigated from the point of the BC: the depth of the first reinforcement layer (u), the number of reinforcement layers (N), and the length of the geosynthetic layer (L). In this study, N, L, and u were considered as N = 1, L/B = 6, and u/B = 0.4, respectively (Guido et al., 1986; Omar et al., 1993; Shin et al., 1993; Das and Omar, 1994; Yetimoglu et al., 1994; Vinod et al., 2009; Moghaddas et al., 2010; Cicek et al., 2015). Furthermore, BC increase in both soil cases was investigated for different relative densities (D_r = 0.3 and 0.7).

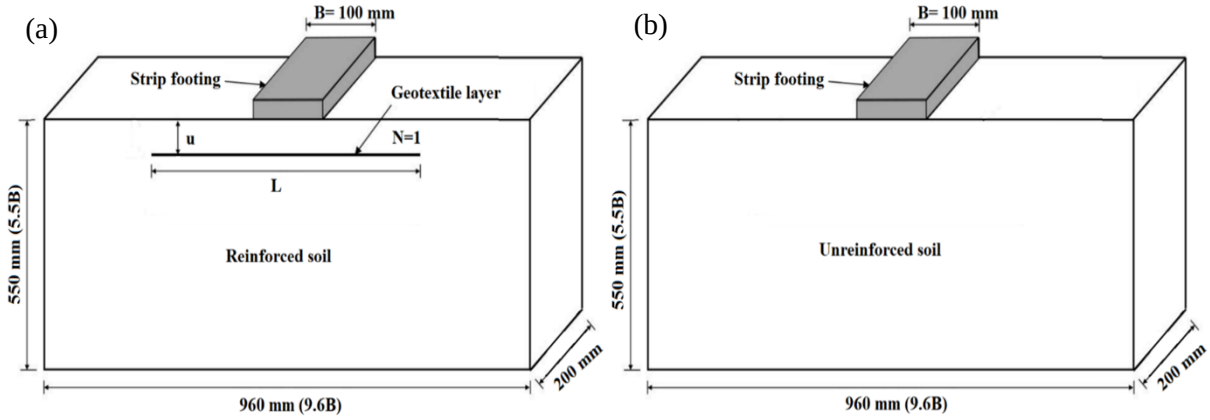

Figure 8. Design Variables for Soil **a.** Reinforced Soil **b.** Unreinforced Soil

For determining the bearing capacity increase due to improving geotextile reinforcement, the experiments illustrated in Table 3 were performed on the strip foundation. A total number of 12 experiments were conducted. The tests are repeated 3 times, and the average of the measurements is defined as the bearing capacity. The results denoted a close match between the results of the trial experiments with a maximum deviation of approximately 3%.

Table 3. Test Program

Test No	Footing	D_r	Soil
$T_{1,2,3}$	Model Strip Foundation	0.3	Unreinforced
$T_{4,5,6}$	Model Strip Foundation	0.3	Reinforced
$T_{7,8,9}$	Model Strip Foundation	0.7	Unreinforced
$T_{10,11,12}$	Model Strip Foundation	0.7	Reinforced

Numerical Analysis

Numerical analysis was conducted to check against the test results. The simulations were conducted by using the PLAXIS 2D. The sizes of the testing tank and the material properties of the sand and geotextile were considered in the PLAXIS 2D software. The Mohr-Coulomb (MC) material model was preferred to reflect the sand and the plain strain case. The MC model is a perfect linear elastic plastic model used to simulate the response of brittle materials. However, this model is used for the simulation of soils due to lesser model parameters measured by simple tests and its simplicity. The MC model requires five parameters such as Poisson's ratio (υ), cohesion (c), friction angle (Ø),

modulus of elasticity (E), and dilatancy angle (ψ). The Poisson's ratios of the loose and dense sand were considered as 0.35 and 0.30, respectively, based on the suggestion for loose and dense density sand from Dutta and Saride (2015). The internal friction angles and elasticity modulus values of the sand were determined with triaxial tests for both loose and dense cases by applying small confining pressures (10, 20 and 40 kPa). A minimal cohesion value was selected because of the numerical stability problem. The parameters of the footing, soil, and reinforcement are presented in Table 4.

Table 4. The Parameters for FE Modelling

Soil Parameters	**Unit**	**Value**
Drainage	-	Undrained
Dry Density, ρ_d (D_r=0.30)	Mg/m^3	1.49
Saturated Density (D_r=0.30)	Mg/m^3	1.62
Dry Density, ρ_d (D_r=0.70)	Mg/m^3	1.66
Saturated Density (D_r=0.70)	Mg/m^3	1.78
Internal Friction Angle, ϕ (D_r=0.30)	Degrees	38.00
Internal Friction Angle, ϕ (D_r=0.70)	Degrees	45.00
Poisson's Ratio, υ (D_r=0.30)	-	0.25
Poisson's Ratio, υ (D_r=0.70)	-	0.30
Dilatancy Angle, ψ (D_r=0.30)	Degrees	8.00
Dilatancy Angle, ψ (D_r=0.70)	Degrees	15.00
Elasticity Modulus, E (D_r=0.30)	kN/m^2	1225
Elasticity Modulus, E (D_r=0.70)	kN/m^2	9500
Cohesion, c	kN/m^2	1.00
Permeability, (k_x=k_y)	m/day	10.00
Footing Parameters	**Unit**	**Value**
Model	-	Strip
Material	-	Steel
Material Model	-	Linear Elastic
Elasticity Modulus, E	kN/m^2	200 x10^6
Poisson's Ratio, υ	-	0.30
EA	kN/m	64e4
EI	kNm^2 /m	85
Reinforcement Parameters	**Unit**	**Value**
Material	-	Geotextile
Ultimate Tensile Strength	kN/m	20.00
EI	kN/m	300

The program of simulations and tests, prepared for specifying the load-settlement response of the soil reinforced with geotextile, is presented in Table 5. The testing procedure was confirmed with Plaxis 2D based on the finite element. Table 5 also presents the mesh details and sizes of FEM.

Table 5. Program for Numerical Analysis

Simulation No	**Foundation**	**D_r**	**Soil**	**Footing width (m)**	**Number of Elements**	**Model Dim. (H-L) (m)**	**Study**
A_1	Model Strip	0.3	Unreinforced	0.1	2960	0.60 -0.96	Verification study
A_2	Model Strip	0.3	Reinforced	0.1	2960	0.60-0.96	
A_3	Model Strip	0.7	Unreinforced	0.1	2960	0.60-0.96	
A_4	Model Strip	0.7	Reinforced	0.1	2960	0.60m-0.96	
A_5	Strip	0.3	Reinforced	0.5	2910	2.75-5.00	Parametric study
A_6	Strip	0.3	Reinforced	1.0	2910	5.50-10.00	
A_7	Strip	0.3	Reinforced	1.5	2910	8.25-15.00	
A_8	Strip	0.3	Reinforced	2.0	2910	11.00-20.00	
A_9	Strip	0.3	Reinforced	2.5	2910	13.75-25.00	
A_{10}	Strip	0.3	Reinforced	3.0	2910	16.50-30.00	
A_{11}	Strip	0.7	Reinforced	0.5	2910	2.75-5.00	
A_{12}	Strip	0.7	Reinforced	1.0	2910	5.50-10.00	
A_{13}	Strip	0.7	Reinforced	1.5	2910	8.25-15.00	
A_{14}	Strip	0.7	Reinforced	2.0	2910	11.00-20.00	
A_{15}	Strip	0.7	Reinforced	2.5	2910	13.75-25.00	
A_{16}	Strip	0.7	Reinforced	3.0	2910	16.50-30.00	

RESULTS AND DISCUSSION

The results of the tests and numerical simulations from the point of the BC increase are presented and examined in this section. A total of 12 experiments and 16 numerical analyses were performed using a model strip foundation. Thus, the Q-s curves of the strip footing were obtained. The BC increases because of the usage of geotextile is quantified from the point of the dimensionless BCR (bearing capacity ratio) factor. Figure 9 illustrates the Q-s curves determined for the strip foundation in the event of unreinforced and reinforced cases with loose conditions. The numerical results were compared with those obtained from experiments; thus, the results of the numerical simulations and the tests were found to be compatible in terms of reflecting the behaviour of the strip footing. The Q-s response was significantly linear in the experiments. The Q-s curves, which are taken from the tests and the numerical analysis in the case of the loose sand for the reinforced and unreinforced soil, agree, and the difference between them is approximately 12%. This difference is within acceptable limits in terms of geotechnical engineering. The material model satisfies the experimental conditions for the loose case. In addition, it has been seen that the geotextile was determined to affect the load-bearing capacity increment of 67% in the case of the loose sand.

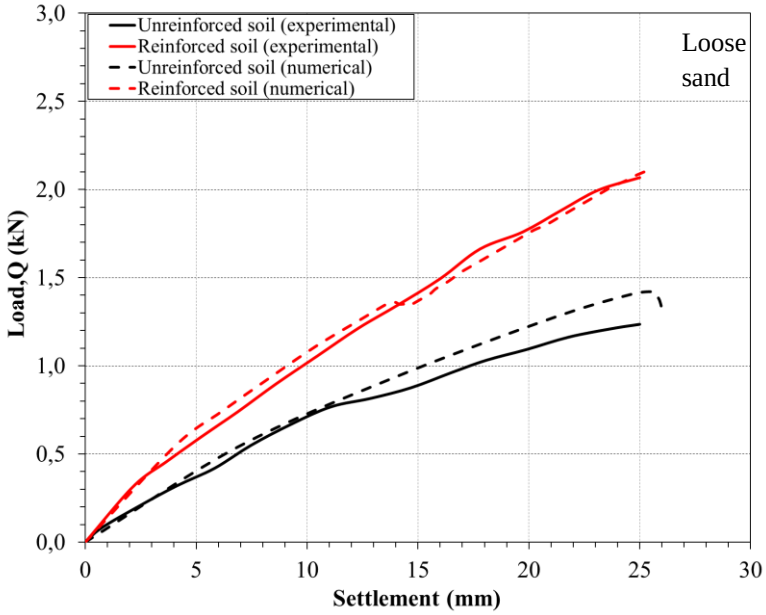

Figure 9. Q-s Curves Determined from Small-Scale Test and Numerical Simulation for $D_r = 0.3$

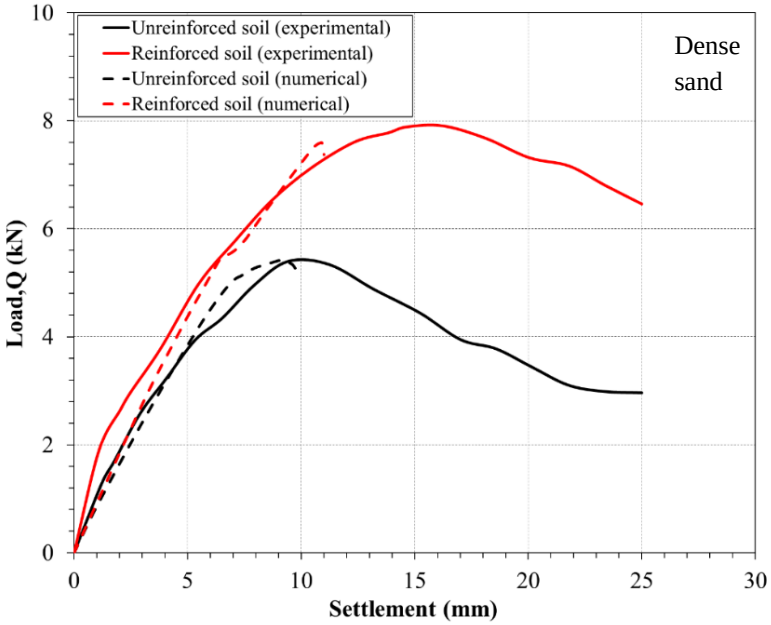

Figure 10. Q-s Curves Determined from Small-Scale Test and Numerical Model for $D_r = 0.7$

Figure 10 illustrates the Q-s curves determined for the footing in event of unreinforced and reinforced dense sand. From comparison of the numerical simulation results with the test results, it is seen that the results of the numerical modellings and the tests were compatible regarding the Q-s behaviours of the model foundation. The Q-s response was significantly non-linear. The Q-s curves, which are obtained in the tests and obtained from the analysis in the case of the dense sand for the reinforced and unreinforced soil, agree, and the difference between them is approximately 5%. This difference is within acceptable limits in terms of geotechnical engineering. It can be said that the material model satisfies the experimental conditions for the dense case until failure. This study was focused on ultimate loads; thus, post-failure behaviour was not discussed at all. In addition, it has been seen that geotextile in the case of dense sand was determined to have an effect on the BC increment of 48%.

Numerical analyses were conducted employing Plaxis 2D software for the footing on the reinforced and unreinforced soils having various relative densities. The vertical settlement determined by the numerical analysis is shown in Figure 11. The significant depth (SG) is usually defined as the depth at which the vertical stress is 10% of the base pressure. The SG is deeper in the case of reinforced sand compared to unreinforced sand, no matter the sand is dense or not.

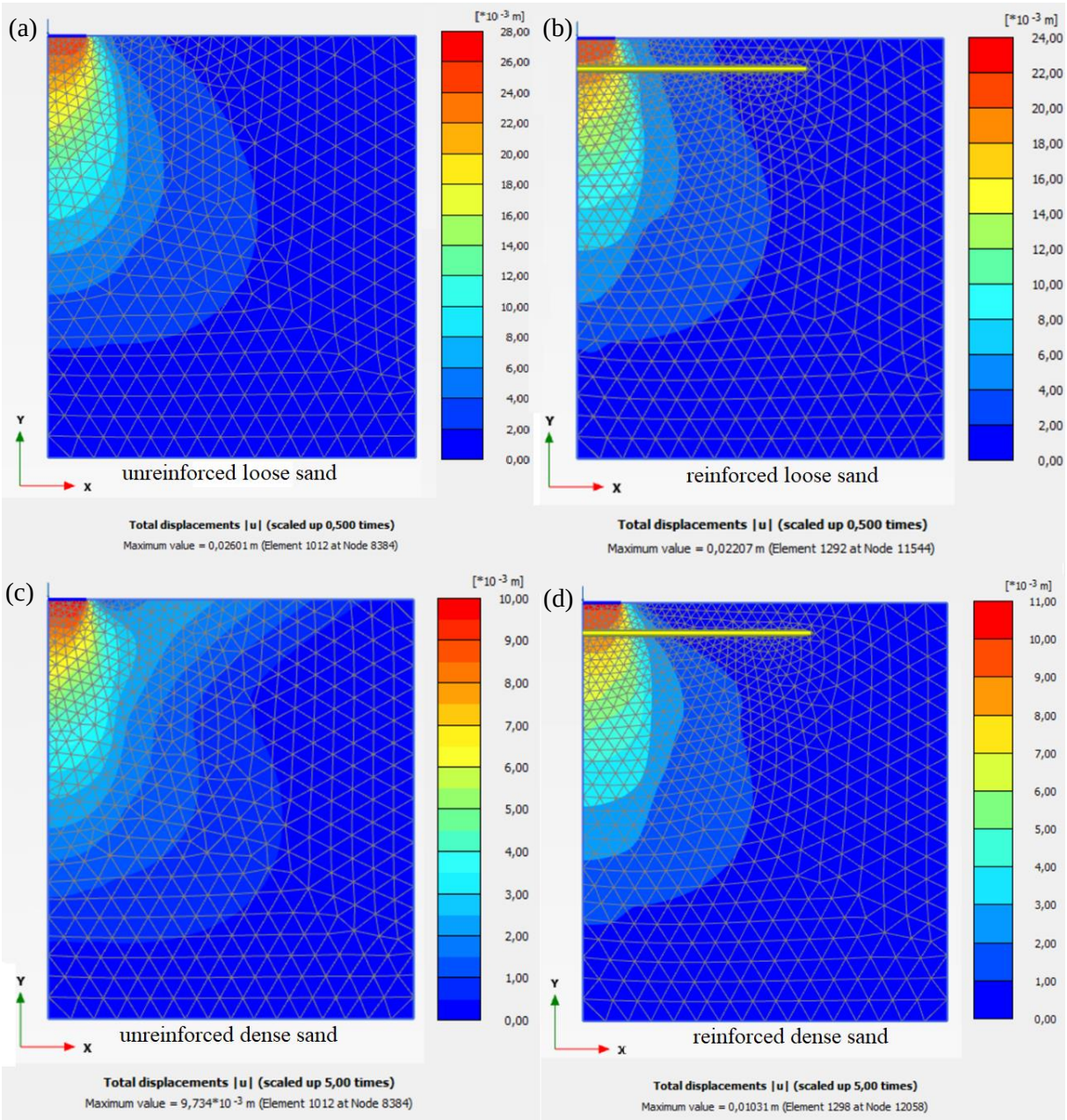

Figure 11. Total Settlements Determined by the Numerical Analysis **a.** Unreinforced Loose Sand **b.** Reinforced Loose Sand **c.** Unreinforced Dense Sand **d.** Reinforced Dense Sand

As a result of the tests performed to determine the BC increment of the sand reinforced with geotextile, it was noticed that relative density is an important parameter from the point of the BC of the unreinforced and reinforced soil. Figure 12 illustrates the BC increase–settlement ratio curve depending on the relative density increase from 0.3 to 0.7 in the event of unreinforced and reinforced soil. It is seen that the BC increase reduces with the improvement in the settlement ratio value up to 25% in the unreinforced and reinforced cases. While the increment from D_r = 0.3 to D_r = 0.7 at low settlement values contributes more to the bearing capacity increment in unreinforced soils, the increment in the relative density at high settlement values contributes more to the BC increment in the reinforced soil. The critical settlement value is about 12%. Beyond the 12% value of the settlement ratio, the geotextile reinforcement can be considered to be mobilised. That is, it can be said that relative density is a significant parameter that affects the increase in BC in both reinforced and unreinforced soils. As the D_r of soil increases from 0.3 to 0.7, while the BC increment of the strip foundation has improved by 875–138% based on the settlement ratio in the unreinforced sand, the BC increment of the foundation has enhanced by 730–212% in the reinforced soil.

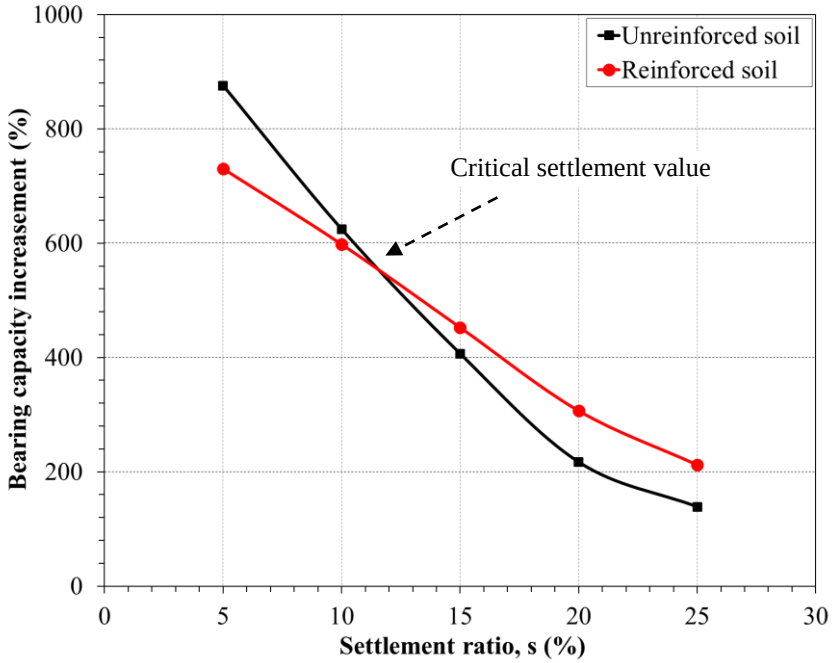

Figure 12. Bearing Capacity Increase Based on Settlement Ratio for Unreinforced Sand and Reinforced Sand

Figure 13 illustrates the variation of BCR depending on the settlement ratio for the reinforced soil. It was determined that this reinforcement in the loose sand improved the BCR of the soil by 1.36–1.67, depending on the settlement ratio. Moreover, the geotextile sheet in the dense sand improved the BCR of the sand by 1.28–2.18, depending on the settlement ratio. For the loose case, while the reinforcement layer contributes more to the increment of BCR at low settlement values, the effect of the geotextile sheet increases slightly as the settlement value increases (beyond 12%).

The parametric study was performed to examine the effect of footing's width on the BC of the reinforced soils by utilising the agreement of the tests and the numerical model. A total of 12 numerical analyses were performed by increasing the strip footing's width from 0.5 m to 3.0 m for the dense and loose reinforced soil. Thus, the bearing capacity-settlement curves of the strip footing with various widths were obtained. Figure 14 illustrates the bearing pressure-footing width curve based on the relative density in the event of the reinforced soil. It is seen that the footing's width is a significant parameter for the BC. As the footing's width increases from B = 0.5m to B = 3m, the BC of the strip footing enhances by 159% in the loose case. For the same increase in the footing's width, the BC increment is 315% in the dense soil.

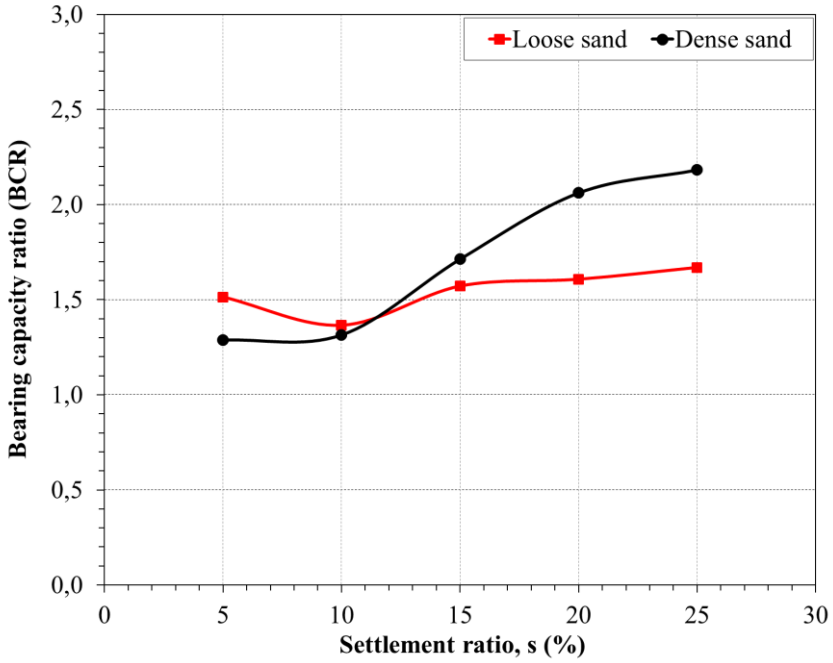

Figure 13. BCR Curves Determined by the Tests for Loose and Dense Cases

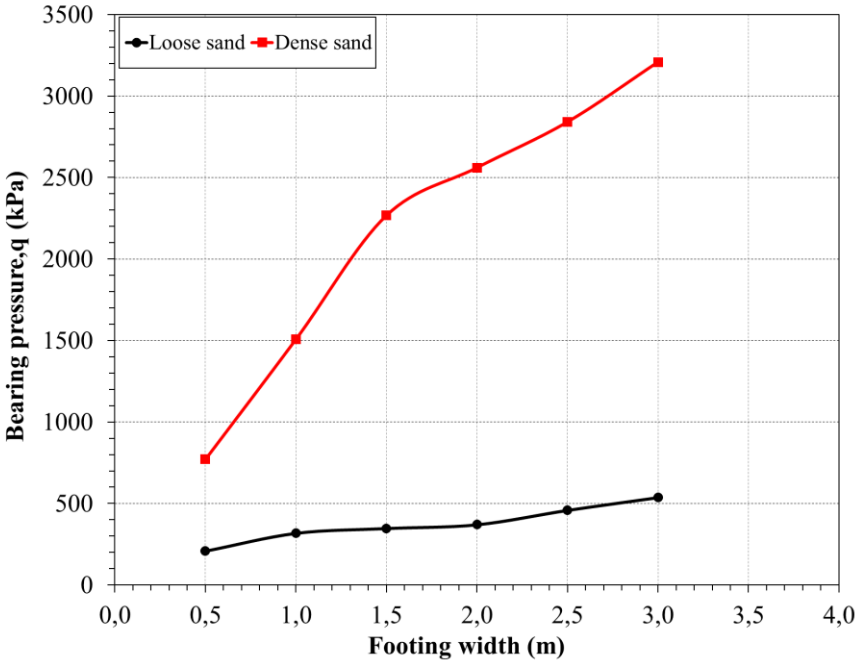

Figure 14. Bearing Pressure-Footing Width Curves Determined by Numerical Analysis

CONCLUSION

The study is intended to detect the BC increment of the sand reinforced with geotextile. For this aim, a testing apparatus has been installed, and the tests have been conducted with the help of small-scale footing on the sand with various relative densities. Besides, this test setup was modelled with PLAXIS 2D software based on finite elements, and numerical analyses were performed. Comparison of the numerical model results with the test results is done. The main results obtained from the experiments and numerical analyses are the following:

- The variation between the results obtained from numerical modelling and tests was in the range of about 5-12%. In other words, the shallow footings can be simulated with enough precision by the 2D-FEM.

- The relative density is an important parameter in the BC increase of the unreinforced and reinforced cases.
- As the D_r increases from 0.3 to 0.7, while the BC increment of the strip footing has improved by 875-138% based on the settlement ratio in the unreinforced sand, the BC increment of the strip footing has advanced by 730-212% in the sand with geotextile.
- The geotextile sheet in the loose case increased the BCR of the soil by 1.36-1.67, depending on the settlement ratio. The geotextile sheet in the dense sand increased the BCR of the soil by 1.28-2.18, depending on the settlement.
- As the width of the footing increased from B=0.5m to B=3m, the load-bearing capacity of the strip footing increased by 159% in the loose case, whereas the BC increment of the footing was 315% in the dense soil. The contribution of geotextile reinforcement to the BC of the strip footings decreases with increase in the footing's width because the BC of unreinforced sand is linearly dependent on footing's width, at least theoretically.

REFERENCES

Abu-Farsakh, M., Chen, Q., M., Sharma, R., (2013). An experimental evaluation of the behavior of footings on geosynthetic-reinforced sand, *Soils Found*, 53(2), 335–348. https://doi.org/10.1016/j.sandf.2013.01.001

Adams, M. T., Collin, J. G., (1997). Large model spread footing load tests on geosynthetic reinforced soil foundations, *Journal of Geotechnical and Geoenvironmental Engineering*, ASCE, 123(1), 66–72. https://doi.org/10.1061/(ASCE)1090-0241(1997)123:1(66)

Asakereh, A., Ghazavi, M., Tafreshi, S.N.M., (2013). Cyclic response of footing on geogrid-reinforced sand with void, *Soils Found*. 53(3), 363–374.

ASTM D-4595, (2017). Standard test method for tensile properties of geotextiles by the wide-width strip method, American Society for Testing and Materials, West Conshohocken.

ASTM D-6913, (2017). Standard test methods for particle-size distribution (gradation) of soils using sieve analysis. American Society for Testing and Materials, West Conshohocken.

ASTM D-854, (2006). Standard test methods for specific gravity of soil solids by water pycnometer. American Society for Testing and Materials, West Conshohocken.

ASTM D4253-16, (2016). Standard test methods for minimum index density and unit weight of soils using a vibratory table. ASTM International, West Conshohocken.

ASTM D4254-16, (2016). Standard test methods for maximum index density and unit weight of soils using a vibratory table. ASTM International, West Conshohocken.

ASTM D3080M-11, (2011). Standard test method for direct shear test of soils under consolidated drained conditions. ASTM International, West Conshohocken.

Ateş, B., Şadoğlu, E., (2014). Donatılı kohezyonsuz zeminlerde düşey gerilme dağılışı, Altıncı Ulusal Geosentetikler Konferansı, İSTANBUL, TÜRKIYE, ss.165-176.

Ateş, B., Şadoğlu, E., (2020). Vertical stress distribution in reinforced sandy soil in plane strain conditions, Teknik Dergi, 31(3), pp.9967-9985. https://doi.org/10.18400/tekderg.449897

Binquet, J., Lee, K. L., (1975). Bearing capacity analysis of reinforced earth slabs, *J. Geotech. Eng. Div*., 101(12), 1257–1276.

Chakraborty, M., Kumar, J., (2014). Bearing capacity of circular foundations reinforced with geogrid sheets, *Soils Found*, 54 (4), 820–832. https://doi.org/10.1016/j.sandf.2014.06.013

Chen, J. F., Guo, X. P., Xue, J. F., Guo, P. H., (2019). Load behaviour of model strip footings on reinforced transparent soils, *Geosynth. Int*., 26(3), 251–260. https://doi.org/10.1680/jgein.19.00003

Chen, J., Guo, X., Sun, R., Rajesh, S., Jiang, S., Xue, J., (2021). Physical and numerical modelling of strip footing on geogrid reinforced transparent sand, *Geotextiles and Geomembranes*, 49(2), 399–412. https://doi.org/10.1016/j.geotexmem.2020.10.011.

Cicek, E., Guler, E., Yetimoglu, T., (2015). Effect of reinforcement length for different geosynthetic reinforcements on strip footing on sand soil, *Soils Found*, 55(4), 661–677. https://doi.org/10.1016/j.sandf.2015.06.001.

Das, B. M., Omar, M. T., (1994). The effects of foundation width on model tests for the bearing capacity of sand with geogrid reinforcement, *Geotech Geol Eng*., 12(3), 133–141. https://doi.org/10.1007/BF00429771

Dutte, T. T. and Saride, S. (2015). Effect of confining pressure, relative density and shear strain on the poisson's ratio of clean sand, 50th Indian Geotechnical Conference.

Gao, Y. X., Zhu, H. H., Ni, Y. F., Wei, C., Shi, B., (2022). Experimental study on uplift behavior of shallow anchor plates in geogrid-reinforced soil. *Geotextiles and Geomembranes*. 50(5), 994–1003. https://doi.org/10.1016/j.geotexmem.2022.06.006.

Ghazavi, M., Lavasan, A. A., (2008). Interference effect of shallow foundations constructed on sand reinforced with geosynthetics. *Geotextiles and Geomembranes*. 26(5), 404–415. https://doi.org/10.1016/j.geotexmem.2008.02.003

Guido, V. A., Chang, D. K., and Sweeney, M. A., (1986). Comparison of geogrid and geotextile reinforced slabs, *Can. Geotech. J*., 23(4), 435–440. https://doi.org/10.1139/t86-073

Hussein M. G., Meguid. M. A., (2019). Improved understanding of geogrid response to pullout loading: insights from three-dimensional finite-element analysis. *Canadian Geotechnical Journal*. 57(2), 277-293. https://doi.org/10.1139/cgj-2018-0384.

Kargar, M., Mir Mohammad Hosseini, S., M., (2016). Influence of reinforcement stiffness and strength on load-settlement response of geocell-reinforced sand bases, *European Journal of Environmental and Civil Engineering*, https://doi.org/10.1080/19648189.2016.1214181.

Kirkpatrick, W. M., Uzuner, B. A., (1975). Measurement errors in model foundations tests. In: Istanbul Conference on Soil Mechanics, Istanbul, pp. 98–106.

Kirkpatrick, W. M., Yanikian, H. A., (1975). Side friction in plane strain tests. In: Proceedings of the Fourth South East Conference On Soil Engineering, Kuala Lumpur, Malaysia, pp. 76–84.

Lai, J., Yang, B. H., (2017). Laboratory testing and numerical simulation of a strip footing on geosynthetically reinforced loose sand. *Journal of Testing and Evaluation*. 45(1), 51–60. https://doi.org/10.1520/JTE20160444.

Lavasan, A. A., Ghazavi, M., (2012). Bearing of closely spaced square and circular footing on reinforced sand. *Soils Found*. 52 (1), 160–167.

Kahraman, M.Ş., Yeşiltepe, Ö., Türedi, Y. ve Örnek, M. (2022). Mikrogrid donatılı zeminde ring temel taşıma kapasitesinin deneysel olarak incelenmesi. *Kahramanmaraş Sütçü İmam Üniversitesi Mühendislik Bilimleri Dergisi*, 25 (4) , 516-527. https://doi.org/10.17780/ksujes.1105191

Michalowski, R.L. and Shi, L. (2003). Deformation patterns of reinforced foundation sand at failure. *Journal of Geotechnical and Geoenviromental Engineering*, ASCE, Vol. 129, pp. 439-449.

Michalowski, R. L., (2004). Limit loads on reinforced foundation soils, *J. Geotech. Geoenviron. Eng*., 130 (4), 381–390.

Moghaddas Tafreshi, S. N., Dawson, A. R., (2010). Comparison of bearing capacity of a strip footing on sand with geocell and with planar forms of geotextile reinforcement. *Geotext Geomembr* 28(1):72–84. https://doi.org/1016/j.geotexmem.2009.09.003

Moroglu, B., Uzuner, B., A., Sadoglu, E., (2005). Behaviour of the model surface strip footing on reinforced sand, *Indian Journal of Engineering and Material Science*, 12 (5), 419–426.

Omar, M., T., Das, B., M., Puri, V., K., Yen, S., C., (1993). Ultimate bearing capacity of shallow foundations on sand with geogrid reinforcement, *Canadian Geotechnical Journal*, 30(3), 545–549. https://doi.org/10.1139/t93-046

Patra, C., R., Das, B., M., Atalar, C., (2005). Bearing capacity of embedded strip foundation on geogrid-reinforced sand, *Geotextiles and Geomembranes*. 23(5), 454–462. https://doi.org/10.1016/j.geotexmem.2005.02.001

Patra, C. R., Das, B. M., Bhoi, M., Shin, E. C., (2006). Eccentrically loaded strip foundation on Geogrid-reinforced sand. *Geotext. Geomembr*. 24 (4), 254–259.

Saha Roy, S., Deb, K., (2017). Bearing capacity of rectangular footings on multilayer geosynthetic-reinforced granular fill over soft soil. *International Journal of Geomechanics*. 17(9), 04017069. https://doi.org/10.1061/(ASCE)GM.1943-5622.0000959.

Shin, E. C., Das, B., M., Puri, V. K., Yen, S. C., Cook, E. E., (1993). Bearing capacity of strip foundation on geogrid reinforced clay. *Geotech Test J ASTM* 16(4):534–541. https://doi.org/10.1520/GTJ10293J

Şadoğlu, E., Uzuner, B. A., (2010). Behaviours of the Model Eccentrically Loaded Strip Footings on Unreinforced and Reinforced Sand, 9th International Congress on Advances in Civil Engineering, Trabzon, Turkey.

Takemura, J., Okamura, M., Suemasa, N. and Kimura, T. (1992). Bearing capacities and deformations of sand reinforced with geogrids. The International Symposium on Earth Reinforcement Practice, November 11-13, Vol. 2, pp. 695-700 Fukuoka, Japan.

Toyosawa, Y., Itoh, K., Kikkawa, N., Yang, J. J., Liu, F., (2013). Influence of model footing diameter and embedded depth on particle size effect in centrifugal bearing capacity tests. *Soils and Foundations*. 53(2), 349-356. https://doi.org/10.1016/j.sandf.2012.11.027.

Useche-Infante, D., Martinez, G. A., Arrúa, P., Eberhardt, M., (2019). Experimental study of behaviour of circular footing on geogrid-reinforced sand. *Geomechanics and Geoengineering*. 17(1), 45–63. https://doi.org/10.1080/17486025.2019.1683621.

Venkateswarlu H., Hegde, A., (2020). Effect of infill materials on vibration isolation efficacy of geocell-reinforced soil beds. *Canadian Geotechnical Journal*. 57(9) 1304-1319. https://doi.org/10.1139/cgj-2019-0135.

Vinod, P., Bhaskar, A. B., Sreehari, S., (2009). Behavior of a square model footing on loose sand reinforced with braided coir rope, Geotext*iles and Geomembranes*, 27(6), 464–474. https://doi.org/10.1016/j.geotexmem.2009.08.001

Wang, J. Q., Zhang, L. L., Xue, J. F., Tang, Y., (2018). Load-settlement response of shallow square footings on geogrid-reinforced sand under cyclic loading. *Geotextiles and Geomembranes*. 46(5), 586–596. https://doi.org/10.1016/j.geotexmem.2018.04.009.

Wayne, M. H., Han, J., Akins, K., (1998). The design of geosynthetic reinforced foundations. In: Proceedings of ASCE's 1998 Annual Convention & Exposition, ASCE Geotechnical Special Publication, 76, pp. 1–18.

Xu, Y., Williams, D. J., Serati, M., Scheuermann, A., Vangsness, T., (2018). Effects of scalping on direct shear strength of crusher run and crusher run/geogrid interface. *Journal of Materials in Civil Engineering*. 30(9). https://doi.org/10.1061/(ASCE)MT.1943-5533.0002411.

Xu, Y., Yan, G., Williams, D. J., Serati, M., Scheuermann, A., Vangsness, T., (2019). Experimental and numerical studies of a strip footing on geosynthetic-reinforced sand. *International Journal of Physical Modelling in Geotechnics*. 20(5), 267–280. https://doi.org/10.1680/jphmg.18.00021.

Yetimoglu, T., Wu, J. T. H., Saglamer, A., (1994). Bearing capacity of rectangular footings on geogrid-reinforced sand, *J. Geotech. Engrg*, 120(12), 2083–2099. https://doi.org/10.1061/(ASCE)0733-9410(1994)120:12(2083)